ADVANCES IN ATMOSPHERIC SCIENCES, VOL. 26, NO. 2, 2009, 229–239

The Linkage between the Pacific-North American Teleconnection Pattern and the North Atlantic Oscillation

SONG Jie*[1,3] (宋 洁), LI Chongyin[1] (李崇银), ZHOU Wen[1,2] (周 文), and PAN Jing[1] (潘 静)

[1] *State Key Laboratory of Numerical Modeling for Atmospheric Sciences and Geophysical Fluid Dynamics (LASG), Institute of Atmospheric Physics (IAP), Chinese Academy of Sciences, Beijing* 100029

[2] *CityU-IAP Laboratory for Atmospheric Sciences, Department of Physics and Materials Science, City University of Hong Kong, Hong Kong*

[3] *Graduate University of Chinese Academy of Sciences, Beijing* 100049

(Received 1 November 2007; revised 3 June 2008)

ABSTRACT

In this study, using the ECMWF reanalysis data, the possible linkage between the Pacific-North American teleconnection pattern (PNA) and the North Atlantic Oscillation (NAO) during boreal winter (December–February) is investigated. The PNA and the NAO pattern are obtained by performing Rotated Empirical Orthogonal Function (REOF) analysis on an anomalous daily mean 300-hPa geopotential height field. The composite daily NAO indices show that the NAO indices are prone to be negative (positive) when the contemporary PNA indices are extremely positive (negative). The correlation coefficients between the daily PNA and NAO indices also confirm that, indeed, there is a significant anti-correlation between the PNA and NAO indices. The correlation peaks at a lag of 0 days (meaning contemporary correlation), and its value is 0.202. Analyses of a newly defined Rossby wave breaking index and diagnostics of the stream function tendency equation indicate that the anti-correlation between PNA and NAO may be caused by the anomalous Rossby wave breaking events associated with the PNA pattern.

Key words: Pacific-North American teleconnection pattern (PNA), North Atlantic Oscillation (NAO), wave breaking

Citation: Song, J., C. Y. Li, W. Zhou, and J. Pan, 2009: The linkage between the Pacific-North American teleconnection pattern and the North Atlantic oscillation. *Adv. Atmos. Sci.*, **26**(2), 229–239, doi: 10.1007/s00376-009-0229-3.

1. Introduction

Many low-frequency variability modes have been discovered in the Northern Hemisphere (NH) extratropics, including the Pacific-North American teleconnection pattern (PNA) and the North Atlantic Oscillation (NAO), being the two most prominent modes among them (Wallace and Gutzler, 1981; Barnston and Livezey, 1987). The PNA has a typical wave-like pattern and covers almost half of the NH. The PNA pattern can modify NH planetary wave amplitudes, perturb the paths of the Pacific storm-track, and also strongly impact the strength and location of the East Asian jet stream. Generally, the PNA is considered as a local phenomena and it has some local influences on the temperature and precipitation anomalies over the north Pacific and North America, especially during the NH cold season (Leathers et al., 1991). Although on an interannual time scale, El Niño/ Southern Oscillation (ENSO) events can impact the variability of the PNA (Trenberth et al., 1998), some studies indicate that the PNA is an essential internal mode of the NH atmospheric variability. The growth of PNA is mainly due to the stationary eddy advection, whereas transient eddy vorticity fluxes also play an important role during some stages of the PNA life cycle (Feldstein, 2002).

The North Atlantic Oscillation (NAO) denotes a

*Corresponding author: SONG Jie, song_jie@mail.iap.ac.cn

seesaw pattern of sea level pressure (SLP) between the Azores and Iceland (Walker, 1924; Walker and Bliss, 1932; van Loon and Rogers, 1978; Hurrell, 1995; Hurrell et al., 2003). Unlike the wave-like PNA pattern, the NAO is a north-south "dipolar" mode and it refers to an out of phase redistribution of atmospheric mass between the Arctic and the subtropical Atlantic as well as the north-south displacement of the mid-latitude jet in the Atlantic sector. The NAO has a strong climatic impact not only on North America/the Atlantic and European regions but also on almost the whole NH domain (Hurrell et al., 2003). The fundamental dynamical processes of the growth and maintenance of the NAO are dominated by the nonlinear processes and the high-frequency (period less than 10 days) transient eddy fluxes that are the main "engine" which drive the growth of the NAO (Feldstein, 2003). Recently, a number of studies considered that the NAO straightly originated from synoptic wave breaking in the north Atlantic (Benedict et al., 2004; Rivière and Orlanski, 2007; Woollings et al., 2008). The anticyclonic (cyclonic) wave breaking corresponded to the positive (negative) phase of the NAO. Some studies also suggested that the variability of the NAO could be affected by the anomalies of the atmospheric circulation in the eastern Pacific, which is the upstream region of the NAO. The composite cycle of positive NAO events show that after an anomalous wave-train propagation across the north Pacific to the east coast of North America, the positive NAO phase develops (Feldstein, 2003). Franzke et al. (2004) pointed out that the latitudinal position of the Pacific storm track was crucial for determining the phase of the NAO. In Woollings et al. (2008)'s analysis, a number of wave breaking events in the Atlantic were preceded by a quasi-stationary Rossby wave train emanating from the eastern Pacific. Rivière and Orlanski (2007) also underscored the important role of the upstream effect in determining the phase of the NAO. Rivière and Orlanski (2007) regional model's results showed that the sign of the NAO indices could be recovered when their regional model was forced with real data at the western boundary (eastern Pacific), which indicated that the phase of NAO was determined by the waves coming from the eastern Pacific.

The PNA, as the most distinct pattern of atmospheric variability located in the eastern Pacific, has dramatic influences on the circulation of the eastern Pacific. Therefore, it is reasonable to hypothesize that there is a linkage between the PNA and the NAO. In fact, some studies have suggested that there is a possible linkage between these two low frequency patterns. Pozo-Vázquez et al. (2001, 2005) examined the SLP anomalies in the north Atlantic region during the different phases of ENSO (El Niño or La Niña). In Pozo-Vázquez et al. (2001, 2005) composite analysis, they found that during La Niña there was a significant anomalous pattern resembling the positive phase of the NAO in the north Atlantic. Besides that, simulations by various ocean-atmosphere coupled models showed that the eastern tropical Pacific SST anomalies are associated with the anomalous SLP, which partly resembles the NAO pattern over the north Atlantic (Zhou et al., 2006, and the references therein). Mokhov and Smirnov (2006) applied a nonlinear method to estimate the coupling between ENSO and the NAO. They inferred that ENSO could affect the variability of the NAO with a confidence probability higher than 95% during the previous half century. Pozo-Vázquez et al. (2001, 2005) suggested that the PNA pattern could be a "bridge" connecting the NAO-like SLP anomaly pattern and the tropical forcing. Reyers et al. (2006) investigated the possible link between the PNA and the NAO in the results of ECHAM4 and ECHAM5 GCM long control runs. Reyers et al. (2006) found that, in the GCMs, there was indeed a significant anticorrelation between the PNA and the NAO (correlation coefficient $r=-0.37$ in ECHAM4; correlation coefficient $r=-0.22$ in ECHAM5). They failed, however, to find any significant correlation between the PNA and the NAO in the reanalysis datasets, except for the period of 1973–1994.

Those aforementioned studies have given us a hint that the two most prominent low-frequency modes in the NH, the PNA and the NAO, have some kind of linkage. However, the linkage between the two patterns in observations is still controversial and unclear. Therefore, in this study, our primary aim is to clarify whether there is a significant linkage between the PNA and the NAO in the reanalysis data. If indeed there is a linkage between them, the possible physical explanation will be discussed. This paper is organized as follows: Datasets and methodology are described in section 2. Observational relationship between the PNA and the NAO indices is presented in section 3 and then a possible mechanism responsible for this linkage is discussed in section 4. Section 5 gives discussion and summary.

2. Data and methodology

In this study, the daily 300-hPa geopotential height fields and Potential Vorticity (PV) at the 350 K isentropic level from the European Centre for Medium-Range Weather Forecasts (ECMWF) ERA-40 reanalysis data (Uppala et al., 2005) are used. The horizontal resolution of data is $2.5^\circ \times 2.5^\circ$. The data spans the years from 1957 to 2002 for the months of October to

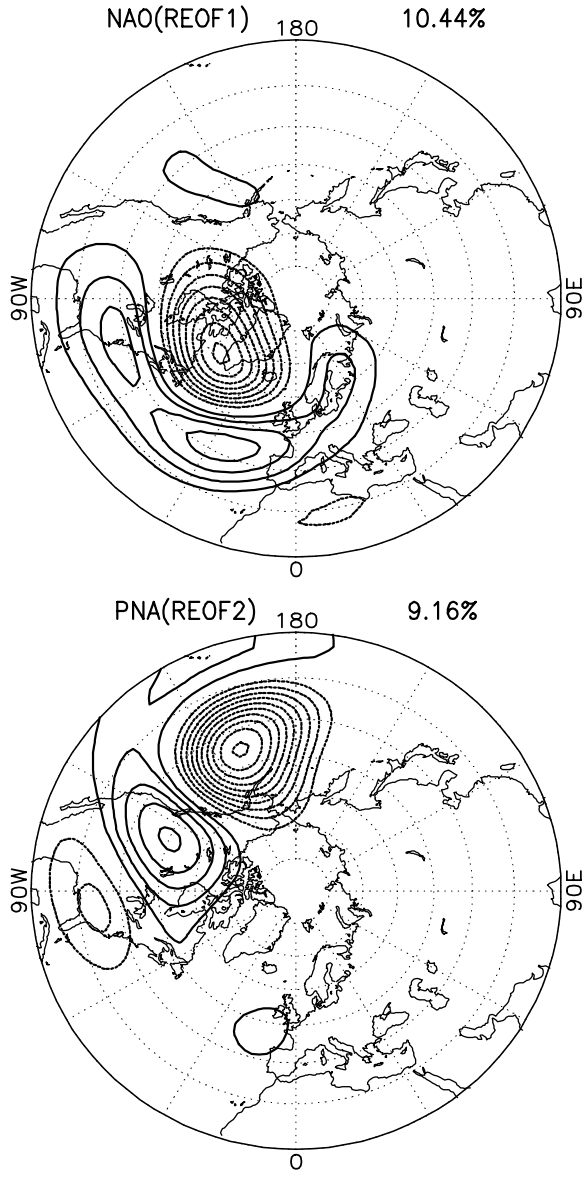

Fig. 1. The North Atlantic Oscillation (NAO, top) and the Pacific-North American teleconnection (PNA, bottom) patterns. The fractional variance is shown in the upper right corner. Full (dashed) contours are positive (negative) and the zero contour is omitted. The interval of the contour is arbitrary.

April. The PNA and the NAO pattern are evident throughout the years, but they are strongly seasonally dependent. During the NH cold season (December–February), their patterns are the most prominent. Hence, in this study, only the relationships between the NAO and the PNA in the cold season are examined, while October, November, March, and April also need to be included if the periods before, or after, an event are to be used.

In order to examine the possible linkage between the PNA and the NAO, clear and exact definitions of the PNA and the NAO patterns are necessary. Unfortunately, there is no "standard" way to define the PNA and the NAO. We follow the definition given by Feldstein (2002, 2003). The spatial structure of NAO and PNA are obtained by applying REOF analysis to the boreal winter (December–January–February, DJF hereafter) daily, unfiltered 300-hPa geopotential height anomalies poleward of 20°N from 1957 to 2002. The term anomaly refers to a deviation from the seasonal cycle, which is defined as every calendar day's climatic average. The first and second REOF are defined as the NAO and the PNA pattern (See Fig. 1). Before we perform the REOF analysis, the data fields will be weighted by the square root of the cosine of the latitude. For the REOF calculation, 15 unrotated EOFs are retained. Also, we found that the NAO and the PNA spatial structures are insensitive to the number of retained unrotated EOFs (retained 12–20 unrotated EOFs are tested). The REOF1 and REOF2 pattern shown in Fig. 1 clearly represent the typical "NAO" and "PNA" spatial structure. The NAO is a north-south out of phase dipole mode with one center over southern Greenland and another very broad center located in the mid-latitude of the north Atlantic. For the PNA, the wave-like four centers are also explicit from the east-central tropical Pacific to North America. The normalized daily NAO and the PNA during the cold season (October–April) are constructed by projecting ECMWF daily unweighted 300-hPa geopotential height field anomalies poleward of 20°N onto the corresponding NAO (REOF1) and PNA (REOF2) loading patterns, respectively. The positive (negative) NAO index polarity refers to the positive (negative) anomaly in the mid-latitude of the North Atlantic and the negative (positive) anomaly over southern Greenland. As for the PNA, the positive (negative) indices indicate that the centers of action over the eastern-central tropical Pacific and northwestern North America are positive (negative), and the other two centers of action have opposite signs.

3. The relationship between the PNA and the NAO

In the presented study, composite and correlation analyses are used to examine the relationship between the NAO and the PNA indices. Any relationship found between the two modes' indices are considered as that between the NAO and the PNA pattern. For the composite analysis, we selected the extremely positive (PNA index$\geqslant$2,268 events) and negative (PNA index$\leqslant -2{,}378$ events) PNA events during the north winter (DJF). We then averaged the NAO indices cor-

responding to extremely positive and negative PNA events for a lag ranging from −60 to +60 days (0 day means the day of the selected extremely positive or negative PNA event, lag $-x$ days means the NAO index leading the extremely positive or negative PNA event x days, lag by $+x$ days means the NAO index lagging the PNA event by days) that were obtained through a composite procedure, respectively (shown in top panel of Fig. 2). In the composite results, we found that the PNA and the NAO indeed have a linkage, that is, the NAO indices are prone to be obviously negative (positive) when the PNA indices are extremely positive (negative), especially during a lag ranging from −10 to +10 days. Some studies have revealed that ENSO has an influence on the variability of the PNA as well as the NAO (Trenberth et al., 1998; Pozo-Vázquez et al., 2001, 2005). In order to consolidate the results of the top panel of Fig. 2 and exclude the possibility that the linkage between the PNA and the NAO is an artifact produced by ENSO, the relationship between the NAO and the PNA in the normal years[a] is also examined (Shown in the bottom panel of Fig. 2). Basically, the total form of results is unchanged except for some minor differences, which indicates that the results of the composite NAO index (top panel of Fig. 2) are substantial and the linkage between the PNA and the NAO is not an artifact created by ENSO.

We also calculated the correlation coefficients between the PNA and the NAO indices for a lag ranging from −60 to +60 days in all years (Shown in the top panel of Fig. 3). In the correlation analysis, 0 days mean that both the PNA and the NAO daily indices are based on 1 December–28 February. Lags $-x$ ($+x$) days mean the NAO index leads (lags) the PNA index by x days. For example, when the correlation is a lag of −10 days (+10 days), the PNA indices are still based on 1 December–28 February, while the NAO indices are based on 21 November–19 February (11 December–10 March). Consistent with the composite results, the correlation shows that there is a significant anti-correlation between the PNA and the

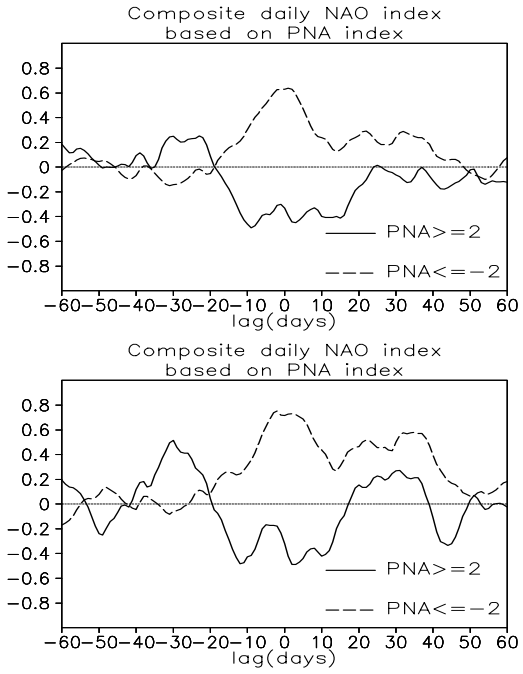

Fig. 2. Composite daily North Atlantic Oscillation (NAO) indices during the extremely positive and negative Pacific-North American teleconnection pattern (PNA) events for a lag ranging from −60 to +60 days in 1957–2002 (top) and in the normal years (bottom). For details see the text.

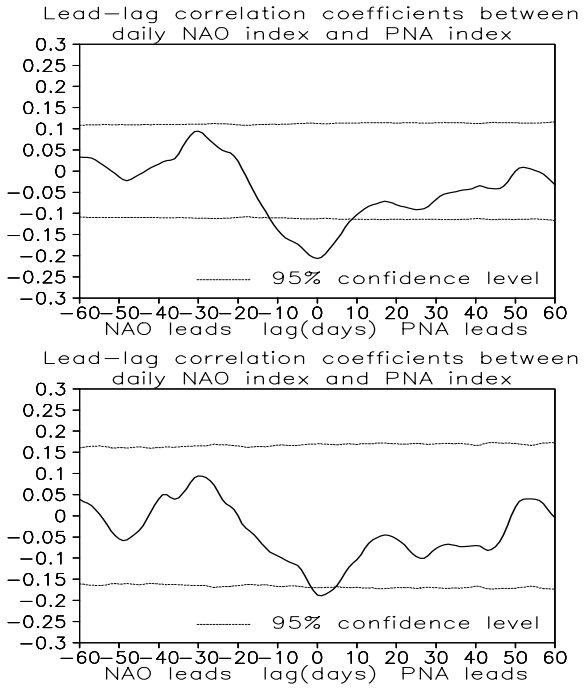

Fig. 3. Correlation coefficients between the daily Pacific-North American teleconnection pattern (PNA) and the North Atlantic Oscillation (NAO) index for a lag ranging from −60 to +60 days in 1957–2002 (top) and in the normal years (bottom). For details see the text.

[a]The normal years are picked out based on the monthly Cold Tongue Index (CTI). The criterion for normal years is to use half a standard deviation ($|\mathrm{CTI}| < 0.5$) of a northern winter (DJF averaged) CTI as the threshold. Therefore, there are 21 normal years from 1957/58 to 2001/02 (58/59, 59/60, 60/61, 61/62, 64/65, 66/67, 71/72, 74/75, 78/79, 79/80, 80/81, 81/82, 83/84, 85/86, 87/88, 89/90, 90/91, 92/93, 93/94, 96/97, and 01/02). The monthly cold tongue index (CTI), defined as the area-averaged (over 6°S–6°N, 180°–90°W) SST anomalies, reflects the variation of the ENSO cycle and is downloaded from the Joint Institute for the Study of the Atmosphere and Ocean at the University of Washington (http://jisao.washington.edu).

NAO indices from a lag −10 to +10 days and the correlation coefficient peaks at a lag of 0 days, with a value of 0.202. For the correlation in the normal years (bottom panel of Fig. 3), the results are basically unchanged, but the number of days that the correlation coefficients exceed the 95% confidence level is decreased dramatically. The anti-correlation between the PNA and the NAO, at least, is still statistically significant at 0 days. We notice that the differences between the correlation coefficients in all years (top panel of Fig. 3) and in the normal years (bottom panel of Fig. 3) are negligible. Therefore, a stricter 95% confidence level, corresponding to a smaller number of effective sample sizes in the normal years, is the reason for the decrease in number of days that the correlation coefficients exceed the 95% confidence level.

4. A possible physical explanation

The simple statistical results presented above confirm that there is a significant linkage between the PNA and the NAO in observations. In this section, a possible physical explanation responsible for the linkage between the PNA and the NAO is discussed.

Noting the fact that most literatures mentioned in section 1 drew the same conclusion: the NAO pattern is closely related to the Rossby wave breaking over the North Atlantic region. From a physical viewpoint, the location of the eddy-driven jet is determined by the eddy momentum fluxes, and so, effectively, the phase of the NAO. The eddy momentum fluxes mainly occur in the later stages of a baroclinic wave's life cycle with an irreversible enstrophy cascade to smaller scales, also known as wave breaking. Therefore, the phases of the NAO are closely related to the wave breaking, or in other words, the NAO can be driven by the wave breaking. Some studies also indicated that the circulation anomalies in upstream regions (eastern Pacific) could impact the variability of the NAO. These results give us a physical basis in explaining the linkage between the PNA and the NAO. We hypothesize that the linkage between the PNA and the NAO could be due to the anomalous upstream Rossby wave breaking events produced by the PNA pattern. From the "PV-θ" viewpoint (Hoskins, 1991), Rossby wave breaking means that the quasi-horizontal amplitude of the Rossby wave is so large that PV contours are irreversibly deformed (McIntyre and Palmer, 1983, 1985). Thorncroft et al. (1993) identified two different kinds of ideal wave breaking, anticyclonic (LC-1) and cyclonic (LC-2). The LC-1 (LC-2) wave breaking is characterized by tongues of high PV air being advected anticyclonically (cyclonically) and then inserting equatorward. In order to depict the Rossby wave breaking events well, a new Rossby wave breaking index is introduced in this study (Appendix A gives a detailed description of the Rossby wave breaking index). Figure 4 shows the anomalous LC-1 (top panel) and LC-2 (bottom panel) Rossby wave breaking indices regressed on the daily NAO index at a lag of 0 days (contemporary regression) during the northern winter (DJF) from 1957 to 2002. The anomalous wave breaking index means a deviation from every calendar day's climatic average of the wave breaking index. The numerical value of regression is multiplied by 100, and a positive (negative) value means that the LC-1 or LC-2 wave breaking events occur more (less) frequently there. Consistent with recent studies, the regressive results of Fig. 4 show that the positive and negative phases of the NAO are closely related to anticyclonic and cyclonic wave breaking events, respectively. The positive (negative) phase of the NAO is associated with a significantly more (less) frequent occurrence of the LC-1 wave breaking event over the mid-latitude of the Atlantic, and a less (more) frequent occurrence of the LC-2 wave breaking event over the North Atlantic. Figure 5 is the same as Fig. 4 but for the PNA index. The positive PNA is associated with a dipole (tripole)-like anomalous LC-1 (LC-2) wave breaking event pattern over the eastern Pacific. In a sense, these patterns reflect the Pacific storm track twisted by the PNA. Obviously, the anomalous wave breaking events associated with the PNA are mainly situated in the eastern Pacific, while the PNA also has an influence on the occurrence of the wave breaking in the North Atlantic/North America. The positive phase of the PNA corresponds to less LC-1 wave breaking events in the mid-latitude (20°–30°N) of the North Atlantic/North America and more LC-1 wave breaking events in the middle-high latitude (30°–55°N) of the North Atlantic/North America. Consulting the results of Fig. 4, this kind of anomalous wave breaking distribution makes against (for) the formation of the positive (negative) phase of the NAO. Therefore, this is a possible explanation for the observed fact that the NAO indices tend to have opposite signs during the extreme phases of the PNA (see Figs. 2 and 3).

The regressive results of the wave breaking index give us a qualitative explanation of the anti-correlation relationship between the PNA and the NAO. In order to validate our suggestion that the anomalous Rossby wave breaking events aroused by the PNA can impact the variability of the NAO, the stream function tendency equation diagnostic method is used. The stream function tendency equation (see Appendix B) was first presented by Cai and van den Dool (1994). Feldstein (1998, 2002, 2003) analyzed the temporal evolution of the PNA and the NAO pattern in a GCM by using

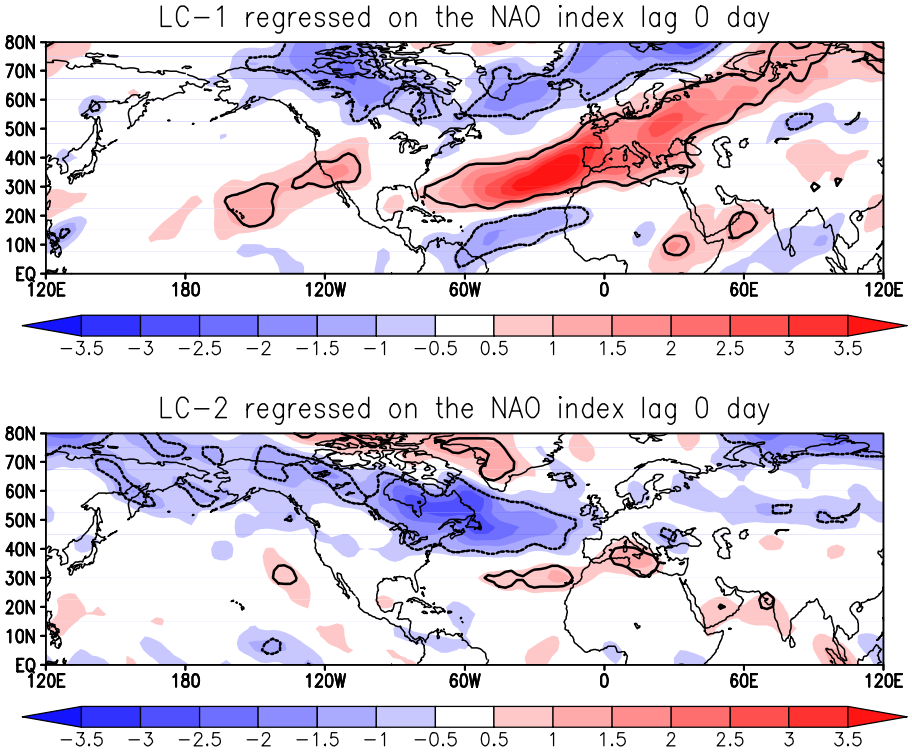

Fig. 4. The anomalous LC-1 (top panel) and LC-2 (bottom panel) Rossby wave breaking indices contemporarily regressed on the daily North Atlantic Oscillation (NAO) index. Areas encircled by the solid and dashed lines denote statistic significance exceeding the 95% confidence level based on the t-test.

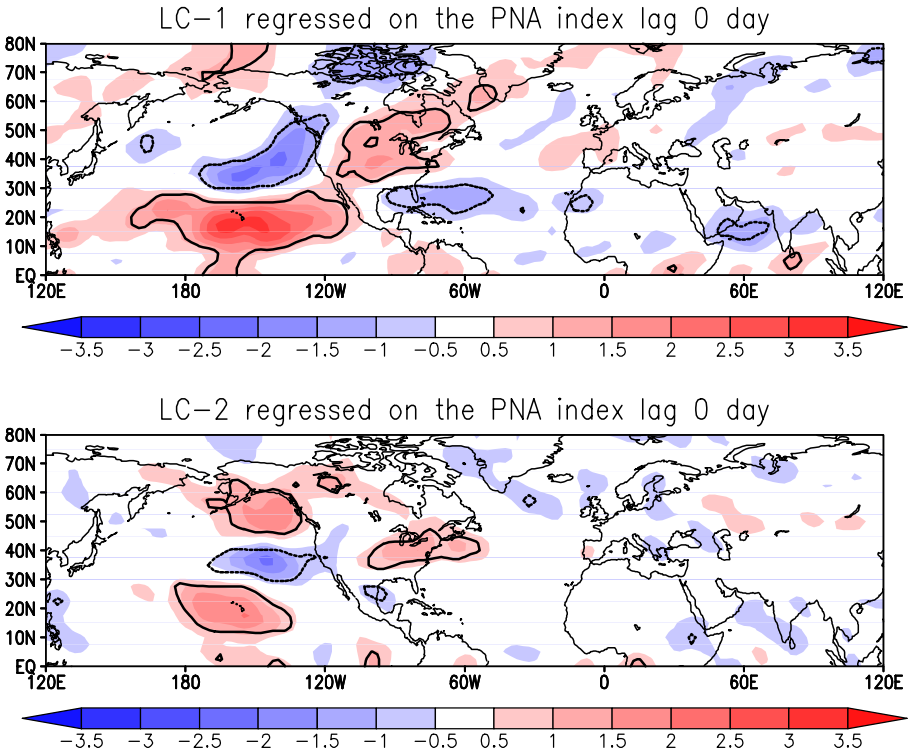

Fig. 5. Same as Fig. 4 but for the Pacific-North American teleconnection pattern (PNA) index.

this diagnostic method. This method, in fact, uses a nearly complete vorticity equation to diagnose the tendency components of the low-frequency anomalies, quantitatively, including the linear and nonlinear processes. Figure 6 shows the nonlinear high-frequency wave interaction term (ξ_6) forcing (the term ξ_6 can represent the eddy vorticity forcing corresponding to wave breaking events approximately), expressed by a stream function tendency regressed on the daily PNA index at a lag of 0 days (contemporary regression) during the northern winter (DJF) from 1957 to 2002. The regressive results show that there is a notable high-frequency transient eddy vorticity forcing associated with the PNA in the north Pacific. A substantial negative stream function tendency center in the north-eastern Pacific strongly projects onto one of the PNA action centers, which is located south of the Aleutian Islands. The PNA can be explained as a Rossby wave train triggered by the tropical forcing and propagating into the middle latitudes, due to linear dispersion (Hoskins and Karoly, 1981). The results of Fig. 6 indicate that the forced Rossby wave train tends to perturb the synoptic waves (high-frequency transient eddy) in the middle latitudes where the activities of the synoptic waves are very intense. On the other hand, the disturbed transient eddy can also significantly enhance the remote response in the mid-latitudes. This is a well known two-way interaction between the transient eddy and the low-frequency pattern, which plays an important role in the formation of mid-latitude circulations. From Fig. 6, we notice that the high-frequency transient eddy forcing associated with positive phase of the PNA produces an anomalous positive stream function tendency in the high latitudes of the North Atlantic. It is plainly disadvantageous (advantageous) for the formation of the positive (negative) phase of the NAO. Therefore, the results of Fig. 6 are helpful to explain why there is an anti-correlation between the PNA and the NAO.

5. Conclusions and discussion

The possible linkages between the PNA and the NAO are examined in the present study. The results of composite and correlation analyses show that there is a significant anti-correlation between the PNA and the NAO from a lag of −10 to +10 days. When the PNA index is extremely positive (negative), the corresponding NAO index tends to be negative (positive). The results reported in this study validate the suggestions proposed by recent studies that there are some linkages between the PNA and the NAO. In fact, the anti-correlation between the PNA and the NAO could also be detected from the 300-hPa zonal wind anomalies patterns associated with the PNA. Figure 7 shows the 300-hPa zonal wind anomalies regressed on the daily PNA index at a lag of 0 days (contemporary regression) and it has a typical quadruple pattern from the eastern Pacific to North America. There are negative zonal wind anomalies poleward of 50°N and positive zonal wind anomalies equatorward of 50°N in the eastern Pacific (negative over positive). On the contrary, anomalous zonal wind fields in North America are positive over negative and extend to the North Atlantic region. This kind of anomalous zonal wind pattern corresponds to the negative phase of the NAO. A possible mechanism that can account for this relationship is also discussed. The anomalous Rossby wave breaking events in the North Atlantic/North America, triggered by the PNA, are considered as the reason explaining the anti-correlation between the PNA and the NAO. It is found that the positive phase of the PNA is associated with more frequent anticyclonic wave breaking events occurring in the high

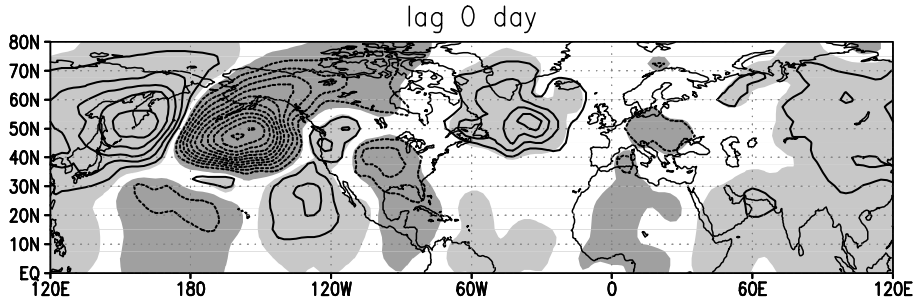

Fig. 6. The high-frequency wave interaction term (ξ_6) forcing expressed by a stream function tendency regressed on the daily Pacific-North American teleconnection pattern (PNA) index at a lag of 0 days during winter (DJF) from 1957 to 2002. Shading denotes statistical significance exceeding the 95% confidence level estimated by a student t-test. Contour intervals are 2 $m^2\ s^{-2}$, zero contours are omitted, and negative contours are dashed.

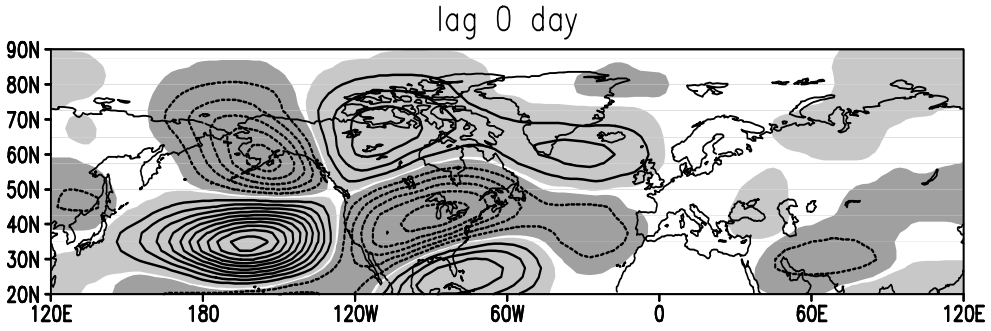

Fig. 7. The 300-hPa zonal wind anomalies regressed on the daily Pacific-North American teleconnection pattern (PNA) index at a lag of 0 days during winter (DJF) from 1957 to 2002. Shading denotes statistical significance exceeding the 95% confidence level estimated by a student t-test. Contour intervals are 1 m s^{-1}, zero contours are omitted, and negative contours are dashed.

latitudes of the North Atlantic/North America and less frequent anticyclonic wave breaking events occurring in the middle-low latitudes of the North Atlantic. This kind of anomalous wave breaking distribution favors the growth of the negative phase of the NAO instead of the positive phase of the NAO. More detailed calculation of the high-frequency wave interaction term (ξ_6, also known as transient eddy vorticity forcing), which roughly represents the eddy vorticity forcing produced by anomalous wave breaking events in the stream function tendency equation, shows that the anomalous wave breaking triggered by the positive (negative) phase of the PNA give rise to an anomalous positive (negative) stream function tendency pattern in the high latitudes of the North Atlantic. This will go against (for) the emergence of the positive (negative) phase of the NAO.

The anomalous wave breaking in North America/North Atlantic associated with the PNA could be due to different baroclinic waves' life cycles influenced by many physical processes. The barotropic meridional shear has been proven to have notable effects on the baroclinic waves' life cycles, that is, the anticyclonic (cyclonic) wave breaking events tend to occur in the regions where anticyclonic (cyclonic) shear is prevalent (Simmons and Hoskins, 1980; Thorncroft et al., 1993; Hartmann and Zuercher, 1998). Actually, in North America, there is anomalous meridional shear brought by the anomalous zonal wind associated with the PNA: anticyclonic shear appears in the high latitudes (means more frequent anticyclonic wave breaking events might occur there) and cyclonic shear appears in the middle-low latitudes (less frequent anticyclonic wave breaking). This is consistent with the results of Fig. 5. Therefore, we hypothesize that the barotropic meridional shear associated with the PNA pattern plays an important role in the formation of the anomalous wave breaking. However, we cannot rule out the effect of other factors on the baroclinic waves' life cycles, such as, changes in the upstream baroclinicity through the advection of warm and moist air from the Gulf of Mexico and cold air from Canada by the PNA (Reyers et al., 2006), or simply the steering effects of the low frequency pattern on the synoptic waves (Branstator, 1995). Recently, the results of a theoretical model proposed by Luo et al. (2008) indicated that the low frequency pattern (in their study the low frequency pattern is the NAO or the blocking circulation) is an outcome through the interaction between synoptic scale waves (high frequency transient eddy) and planetary scale waves. In the evolutional progress of the low frequency pattern, the synoptic waves interact with the planetary waves and the wave breaking inevitably takes place. Hence, there is also a possibility that the anomalous wave breaking events shown in Fig. 5 are a spontaneous result of the interaction between the synoptic waves and the planetary waves associated with the PNA. Whatever, the cause of the anomalous wave breaking, is a topic that needs further research.

The anti-correlation between the PNA and the NAO reported in this study, in fact, also provides a number of potential targets that deserve further research. We are especially interested in investigating the role that tropical forcings, such as SST and convection anomalies, play in the variability of NAO. Hurrell et al. (2004) and Hoerling et al. (2004) argued that the well known linear trend of the NAO index over the last half of the 20th Century (e.g., Hurrell, 1995) was a response to the historical evolution of the SST forcing, especially the tropical Indian Ocean forcing. In their ensembles of numerical experiments, they found that the warm tropical Indian Ocean SST anomalies gave rise to a negative phase PNA-like response in the

eastern Pacific/North American region and then an appreciable positive phase NAO-like response emerged in the North Atlantic. The Madden-Julian oscillation (MJO) is also an important tropical atmospheric phenomenon (Madden and Julian, 1971), whose influence on extratropical circulations have also been extensively examined (Li and Qin, 1991; Hsu, 1996). Does the MJO, like the tropical SST anomalies, influence the variability of the NAO? This question is intriguing and is a future research plan. We believe that, for examining the relationship between the MJO and the NAO, the emphasis should be put on the understanding of synoptic eddy feedbacks associated with changes in the Pacific/Atlantic storm tracks.

Acknowledgements. This work is supported by the State Key Development Progeam for Basic Research of China (Grant No. 2007CB411805) and the National Natural Science Foundation of China (Grant No. 40675051).

APPENDIX A

Rossby Wave Breaking Index

In this study, the basic idea of the Rossby wave breaking index is derived from the work of Woollings et al. (2008). Here we extend their index simply by dividing a wave breaking event into LC-1 and LC-2 types. The Rossby wave breaking index is constructed as follows. First, we search for the reversal in the sign of the meridional gradient of the PV at the 350 K isentropic level on every point of the grid. In order to avoid the disturbance caused by small scale waves (smaller than Rossby waves), the PV field is filtered by performing a Fourier transform, so that, only the information of 0–15 waves is retained. Here, the 350 K isentropic level is chosen because this level is located in the center of the so-called "middle world" where isoentropes crossing the tropopause have not struck the Earth's surface yet (Hoskins, 1991). We define a wave breaking event occurring in this grid when there is a reversal in the sign of the meridional gradient of the PV, namely, $\partial(\mathrm{PV})/\partial(\mathrm{latitude})<0$. Then, the wave breaking event is divided into two classes: anticyclonic (LC-1) and cyclonic (LC-2). When the latitudinal gradient of the PV, namely, $\partial(\mathrm{PV})/\partial(\mathrm{longitude})>0$, the wave breaking event is defined as the LC-1 type, otherwise if $\partial(\mathrm{PV})/\partial(\mathrm{longitude})<0$, the wave breaking event is defined as the LC-2 type. The climatic distribution of the LC-1 and LC-2 Rossby wave breaking events during the cold season (October–April) from 1957 to 2002 in the NH (not shown) indicates that anticyclonic (LC-1) wave breaking events mainly occur at the equatorward region of the climatological jet, where anticyclonic shear is prevalent. For the cyclonic (LC-2) wave breaking events, the maximum is situated in the North Pacific and the North Atlantic, also at the poleward region of the climatological jet where cyclonic shear is prevalent. Diao et al. (2006) indicated that the blocking events are closely related to the cyclonic wave breaking events. Therefore, it is not surprising to notice the North Pacific and the North Atlantic as the locations where the LC-2 wave breaking events are prevalent are also the locations where the blocking events occur, predominantly. The spatial distribution of wave breaking events is also consistent with the results of Thorncroft et al. (1993). The LC-1 (LC-2) wave breaking tends to occur in the equatorward (poleward) region of the main westerly jet, which indicates that our definition of the wave breaking events is reasonable.

APPENDIX B

Stream Function Tendency Equation

The stream function tendency equation is written as follow,

$$\frac{\partial \psi_{\mathrm{l}}}{\partial t} = \sum_{i=1}^{8} \xi_i + R$$

and

$$\begin{aligned}
\xi_1 =& \nabla^{-2}\left[-(v_{\mathrm{r,l}} + v_{\mathrm{d,l}})\frac{1}{a}\frac{df}{d\theta}\right] ,\\
\xi_2 =& \nabla^{-2}(-[\overline{V_{\mathrm{r}}}]\cdot\nabla\xi_{\mathrm{l}} - V_{\mathrm{r,l}}\cdot\nabla[\overline{\xi}])+\\
& \nabla^{-2}(-[\overline{V_{\mathrm{d}}}]\cdot\nabla\xi_{\mathrm{l}} - V_{\mathrm{d,l}}\cdot\nabla[\overline{\xi}]) ,\\
\xi_3 =& \nabla^{-2}(-\overline{V_{\mathrm{r}}^*}\cdot\nabla\xi_{\mathrm{l}} - V_{\mathrm{r,l}}\cdot\nabla\overline{\xi^*})+\\
& \nabla^{-2}(-\overline{V_{\mathrm{d}}^*}\cdot\nabla\xi_{\mathrm{l}} - V_{\mathrm{d,l}}\cdot\nabla\overline{\xi^*}) ,\\
\xi_4 =& \nabla^{-2}\{-(f+\overline{\xi})\nabla\cdot V_{\mathrm{d,l}} - \xi_{\mathrm{l}}\nabla\cdot\overline{V_{\mathrm{d}}}\} ,\\
\xi_5 =& \nabla^{-2}(-V_{\mathrm{r,l}}\cdot\nabla\xi_{\mathrm{l}})_{\mathrm{l}} + \nabla^{-2}\{-\nabla\cdot(V_{\mathrm{d,l}})\xi_{\mathrm{l}}\}_{\mathrm{l}} ,\\
\xi_6 =& \nabla^{-2}(-V_{\mathrm{r,h}}\cdot\nabla\xi_{\mathrm{h}})_{\mathrm{l}} + \nabla^{-2}\{-\nabla\cdot(V_{\mathrm{d,h}}\xi_{\mathrm{h}})\}_{\mathrm{l}} ,\\
\xi_7 =& \nabla^{-2}(-V_{\mathrm{r,l}}\cdot\nabla\xi_{\mathrm{h}})_{\mathrm{l}} + \nabla^{-2}\{-\nabla\cdot(V_{\mathrm{d,l}}\xi_{\mathrm{h}})\}_{\mathrm{l}}+\\
& \nabla^{-2}(-V_{\mathrm{r,h}}\cdot\nabla\xi_{\mathrm{l}})_{\mathrm{l}} + \nabla^{-2}\{-\nabla\cdot(V_{\mathrm{d,h}}\xi_{\mathrm{l}})\}_{\mathrm{l}} ,\\
\xi_8 =& \nabla^{-2}\{-K\cdot\nabla\times(\omega_{\mathrm{l}}\partial\overline{V}/\partial P)\}+\\
& \nabla^{-2}\{-K\cdot\nabla\times(\overline{\omega}\partial V_{\mathrm{l}}/\partial P)\}+\\
& \nabla^{-2}\{-K\cdot\nabla\times(\omega'\partial V'/\partial P)\}_{\mathrm{l}} ,
\end{aligned}$$

where ψ is the stream function, ξ is the relative vorticity, v is the horizontal wind vector, ν is the meridional wind component, ω is the vertical wind component, a is the earth's radius, f is the Coriolis parameter, and

θ is the latitude. The term R corresponds to a residual, including physical progresses that have been neglected. The subscripts r and d denote the rotational and divergent components of the horizontal wind, respectively. The subscripts h and l indicate the data is 10-day high- and low-pass filtered, respectively. The seasonal cycle, which is defined as the time mean of each calendar day, is removed when the low-pass filter is applied. The time mean is denoted by an overbar and the deviations from time mean are represented by a prime. The zonal average is denoted by square brackets and deviations from the zonal mean are denoted by an asterisk.

The dynamic meaning of each term ξ_i is briefly illuminated as follow. ξ_1 corresponds to planetary vorticity advection by the anomalies, ξ_2 (ξ_3) correspond to relative vorticity advection of the interaction of the anomalies with the zonally symmetric (asymmetric) climatological flow, ξ_4 correspond to the divergence term, ξ_5 (ξ_6) correspond to the interaction among low- (high-) frequency transient eddies. ξ_7 and ξ_8 represent the interaction between high- and low- frequency transient eddies and the tilting terms. The last two terms make a negligible contribution to the stream function tendency.

REFERENCES

Barnston, A. G., and R. E. Livezey, 1987: Classification, seasonality and persistence of low-frequency atmospheric circulation patterns. *Mon. Wea. Rev.*, **115**, 1083–1126.

Benedict, J., S. Lee., and S. B. Feldstein., 2004: Synoptic view of the North Atlantic Oscillation. *J. Atmos. Sci.*, **61**, 121–144.

Branstator, G., 1995: Organization of storm track anomalies by recurring low-frequency circulation anomalies. *J. Atmos. Sci.*, **52**, 207–226.

Cai, M., and H. M. van den Dool, 1994: Dynamical decomposition of low-frequency tendencies. *J. Atmos. Sci.*, **51**, 2086–2100.

Diao, Y., J. P. Li, and D. Luo, 2006: A new blocking index and its application: Blocking action in the Northern Hemisphere. *J. Climate*, **19**, 4819–4839.

Feldstein, S. B., 1998: The growth and decay of low-frequency anomalies in a GCM. *J. Atmos. Sci.*, **55**, 415–428.

Feldstein, S. B., 2002: Fundamental mechanisms of the growth and decay of the PNA teleconnection pattern. *Quart. J. Roy. Meteor. Soc.*, **128**, 775–796.

Feldstein, S. B., 2003: The dynamics of NAO teleconnection pattern growth and decay. *Quart. J. Roy. Meteor. Soc.*, **129**, 901–924.

Franzke, C., S. Lee, and S. B. Feldstein, 2004: Is the North Atlantic Oscillation a breaking wave? *J. Atmos. Sci.*, **61**, 145–160.

Hartmann, D. L., and P. Zuercher, 1998: Response of baroclinic life cycles to barotropic shear. *J. Atmos. Sci.*, **55**, 297–313.

Hoerling, M. P., J. W. Hurrell, T. Xu, G. T. Bates, and A. Phillips, 2004: Twentieth century North Atlantic climate change. Part II: Understanding the effect of Indian Ocean warming. *Climate. Dyn.*, **23**, 392–405.

Hoskins, B. J., 1991: Towards a PV-θ view of the general circulation. *Tellus*(B), **43**, 27–35.

Hoskins, B. J., and D. J. Karoly, 1981: The steady linear response of a spherical atmosphere to thermal and orographic Forcing. *J. Atmos. Sci.*, **38**, 1179–1196.

Hsu, H. H., 1996: Global view of the intraseasonal oscillation during northern winter. *J. Climate*, **9**, 2386–2406.

Hurrell, J. W., 1995: Decadal trends in the North Atlantic oscillation: Regional temperatures and precipitation, *Science*, **269**, 676–679.

Hurrell, J. W., Y. Kushnir, G. Ottersen, and M. Visbeck, 2003: The North Atlantic Oscillation: Climate significance and environmental impact. *Geophysical Monograph*, doi: 10.1029/134GM01.

Hurrell, J. W., M. P. Hoerling, A. S. Phillips, and T. Xu, 2004: Twentieth century North Atlantic climate change. Part I: Assessing determinism. *Climate Dyn.*, **23**, 371–389.

Leathers, D. J., B. Yarnal, and M. A. Palecki, 1991: The Pacific/North American teleconnection pattern and United States climate. Part I: Regional temperature and precipitation associations. *J. Climate*, **4**, 517–528.

Li, C. Y., and Z. Qin, 1991: Global atmospheric low frequency teleconnection. *Progress in Natural Science*, **1**, 447–452.

Luo, D., T. Gong, and Y. Diao, 2008: Dynamics of eddy-driven low-frequency dipole modes. Part IV: Planetary and synoptic wave-breaking processes during the NAO life cycle. *J. Atmos. Sci.*, **65**, 737–765.

Madden, R. A., and P. R. Julian, 1971: Detection of a 40–50 Day Oscillation in the zonal wind in the Tropical Pacific. *J. Atmos. Sci.*, **28**, 702–708.

McIntyre, M. E., and T. N. Palmer, 1983: Breaking planetary waves in the stratosphere. *Nature*, **305**, 593–600.

McIntyre, M. E., and T. N. Palmer, 1985: A note on the general concept of wave breaking for Rossby and gravity waves. *Pure. Appl. Geophys.*, **123**, 964–975.

Mokhov, I. I., and D. A. Smirnov., 2006: El Niño-Southern Oscillation drives North Atlantic Oscillation as revealed with nonlinear techniques from climatic indices. *Geophys. Res. Lett.*, **33**. doi: 10.1029/2005GL024557.

Pozo-Vázquez, D., M. J. Esteban-Parra, F. S. Rodrigo, and Y. Castro-Díez, 2001: The association between ENSO and winter atmospheric circulation and temperature in the North Atlantic region. *J. Climate*, **16**, 3408–3420.

Pozo-Vázquez, D., S. R. Gámiz-Fortis, J. Tovar-Pescador, M. J. Esteban-Parra, and Y. Castro-Díez, 2005: North Atlantic winter SLP anomalies based on the

autumn ENSO state. *J. Climate*, **18**, 97–103.

Reyers, M., U. UIbrich, M. Christoph, J. G. Pinto, and M. Kerschgens, 2006: A mechanism of PNA influence on NAO. *Geophysical Research Abstracts*, **8**, 10703.

Rivière, G., and I. Orlanski., 2007: Characteristics of the Atlantic storm-track eddy activity and its relation with the North Atlantic Oscillation. *J. Atmos. Sci.*, **64**, 241–266.

Simmons, A. J., and B. J. Hoskins, 1980: Barotropic influences on the growth and decay of nonlinear baroclinic waves. *J. Atmos. Sci.*, **37**, 1679–1684.

Thorncroft, C. D., B. J. Hoskins, and M. E. McIntyre, 1993: Two paradigms of baroclinic-wave life-cycle behaviour. *Quart. J. Roy. Meteor. Soc.*, **119**, 17–55.

Trenberth, K. E., G. W. Branstator, D. Karoly, A. Kumar, N. C. Lau, and C. Ropelewski, 1998: Progress during TOGA in understanding and modeling global teleconnections associated with tropical sea surface temperatures. *J. Geophys. Res.*, **103**, 14291–14324.

Uppala, S. M., and Coauthors, 2005: The ERA-40 reanalysis. *Quart. J. Roy. Meteor. Soc.*, **131**, 2961–3012.

van Loon, H., and J. C. Rogers, 1978: The seesaw in winter temperature between Greenland and northern Europe. Part I: General description. *Mon. Wea. Rev.*, **106**, 296–310.

Walker, G. T., 1924: Correlations in seasonal variations of weather, IX: A further study of world weather. *Memoirs of the India Meteorological Department*, **24**, 275–332.

Walker, G. T., and E. W. Bliss, 1932: World weather V. *Memoirs of the Royal Meteorological Society*, **4**, 53–84.

Wallace, J. M., and D. S. Gutzler, 1981: Teleconnections in the geopotential height field during the Northern Hemisphere winter. *Mon. Wea. Rev.*, **109**, 784–812.

Woollings, T. J., B. J. Hoskins, M. Blackburn, and P. Berrisford, 2008: A new Rossby wave breaking interpretation of the North Atlantic Oscillation. *J. Atmos. Sci.*, **65**, 609–626.

Zhou, T., R. Yu, Y. Gao, and H. Drange, 2006: Ocean-atmosphere coupled model simulation of North Atlantic Interannual variability II: Tropical teleconnection. *Acta Meteorologica Sinica*, **64**, 18–30. (in Chinese)